Materials Research Proceedings 41 (2024) 156-163 https://doi.org/10.21741/9781644903131-17

Processability of aluminum-matrix composite (AMC) by ultrasonic powder atomization

JEDYNAK Angelika[1,a *], HÄRTEL Sebastian[1,b], PIPPIG Robert[2,c] and CHOMA Tomasz[3,d]

[1]Chair of Hybrid Manufacturing, Brandenburg University of Technology Cottbus - Senftenberg, Konrad - Wachsmann – Allee 17, D-03046 Cottbus, Germany

[2]CMMC GmbH, Emilienstrasse 45, D-09131 Chemnitz, Germany

[3]AMAZEMET | Warsaw University of Technology, 27 Jana Pawla II, PL-00-867 Warsaw, Poland

[a]angelika.jedynak@b-tu.de, [b]sebastian.haertel@b-tu.de, [c]robert.pippig@cmmc-engineering.com, [d]tomasz.choma@amazemet.com

Keywords: Additive Manufacturing, Aluminum-Matrix Composite Powder, Ultrasonic Atomization

Abstract. This research presents a comprehensive study on the production of aluminum-matrix composite (AMC) powders using ultrasonic atomization for additive manufacturing (AM). The impact of different heat sources—plasma, arc, and induction melting—was evaluated on the processability and resultant properties of the AMC powders, including morphology, size, and composite structure. Additionally, induction melting was considered in terms of process parameters such as pressure difference, nozzle size, and frequency. The analysis of AMC powder processability revealed that the efficiency of the ultrasonic process depended on the selected heat source. The highest efficiency, nearly 50%, was attained with the induction system. All produced AMC powders exhibited high sphericity, with average sizes ranging from 88.2 to 120 μm. However, the desired composite structure was not achieved under tested conditions due to the decrease in SiC particle content from 20% in the feed material to approximately 3.5% in the final AMC powder. Based on these results, the research highlights the potential and limitations of ultrasonic atomization in AMC powder production, emphasizing the need for further optimization to improve powder quality and process efficiency for broader industrial application in AM.

Introduction

In recent years, the processing of aluminum-matrix composites (AMCs) using additive manufacturing (AM) technology has attracted attention. This is due to its capability to produce highly complex AMC components without the need for tooling and the time-consuming machining required by conventional processes such as casting. However, the available technologies for producing feedstock materials from AMCs for AM still do not ensure their appropriate properties, thus limiting the adaptation of AM for this group of materials on an industrial scale [1,2]. For AMC powders utilized as feedstock materials, achieving a composite structure with a uniform distribution and the desired content of reinforcing particles in the alloy matrix is a critical property for obtaining high mechanical parameters in the final AM components [3,4]. The most common production methods of AMC powders such as gas atomization show that process difficulties in providing the composite structure described above arise already during the melting of the initial material before atomization. For example, these difficulties include the dissolution of reinforcing particles or insufficient homogenization [5]. Overcoming these challenges necessitates the development of alternative technologies to produce AMC powders.

Ultrasonic powder atomization has emerged as a cutting-edge technique for generating a variety of metal powders with exceptional spherical properties on a laboratory scale. This method

harnesses ultrasonic vibrations to disintegrate molten metal, resulting in the formation of fine droplets of metal or metal alloy. These droplets then solidify into finely textured and spherical powder particles. The current configurations of ultrasonic atomizers facilitate the direct melting of the source material through plasma, arc, or induction melting in a crucible [6]. The utilization of heat sources with varying characteristics enables the processing of a wide array of materials. For instance, induction melting aids in mitigating the loss of low-melting elements like magnesium or aluminum. Previous research by the author [7] showcased the applicability of ultrasonic atomization in the production of AMC powder. However, the primary challenge encountered during the atomization process was the partial dissolution of SiC in the aluminum matrix of the AMC powder, due to the high temperatures generated during arc melting. Therefore, the aim of this study is to employ alternative heat sources - plasma and induction melting - to produce AMC powder with desired properties. Additionally, variations in process parameters for induction melting will be investigated.

Materials and methods

In this study, AMC material made from AlSi9Mg aluminum alloy reinforced with 20 vol% SiC particles was investigated, with an average size of SiC particles at 29.2 µm. This material was fabricated through direct vacuum casting, following the procedure developed by CMMC GmbH [8]. The initial microstructure of AMC material is depicted in Fig. 1. The chemical composition of the AlSi9Mg aluminum alloy matrix is provided in Table 1.

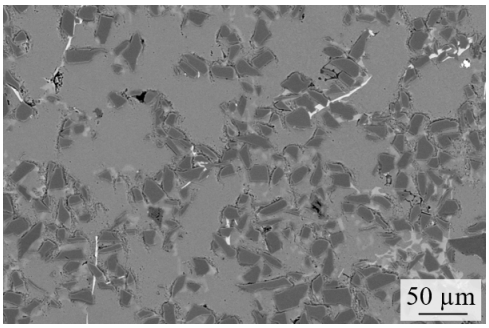

Fig. 1: Initial microstructure of AMC material.

Table 1: Chemical composition of AlSi9Mg alloy in [wt.%] according to the EN AC-43300.

Si	Mg	Fe	Cu	Mn	Zn	Ti	Pb	Al	Others
9.0 - 10.0	0.25 – 0.45	<0.19	<0.05	<0.1	<0.07	<0.15	<0.03	Balance	0.1

Table 2: Ultrasonic atomization process parameters for production of AMC powders.

ATZ no.	Heat source	Frequency, [kHz]	Pressure difference, [mbar]	Nozzle size, [mm]
1111	Arc	35	---	---
1213	Plasma	40	---	---
1203	Induction*	40	500	1.2
1197	Induction*	60	500	1.0
1192	Induction*	60	300	1.0
1195	Induction*	60	300	1.5

* melting in a graphite crucible at a temperature of 1100°C

Ultrasonic atomization processes were carried out using two separate systems. Ultrasonic atomization through induction and plasma melting was conducted at AMAZMENT on the

rePowder system. Ultrasonic atomization using arc melting occurred at 3DLab on the ATOLab+ machine. The process parameters for both systems are detailed in Table 2. Each atomization process was conducted in an atmosphere of pure argon, with an O2 content consistently maintained below 100 ppm. Following the atomization, the powders were sieved with a mesh size under 0.2 mm.

The possibility of processing AMC powder through ultrasonic atomization was determined using the process efficiency values. Process efficiency arises from the correlation between the feedstock material and the quantity of produced powder, according to the equation (1). Based on the documentation prepared during the processes, main process effects were analyzed that could have an impact on the efficiency value.

$$process\ efficiency\ [\%] = \frac{quantitiy\ of\ produced\ powder\ [g]}{quantitiy\ of\ feed\ material\ [g]} * 100 \quad (1)$$

The powder analysis involved scrutinizing the morphology, dimensions, and composite configuration of the atomized AMC powders. Each powder batch was analyzed with approximately one hundred powder particles. To assess powder morphology and particle size, the powder particles were dispersed onto graphite tape and imaged using a scanning electron microscope (SEM) fitted with a Secondary Electron (SE) detector. The SEM SE images were analyzed to determine particle size and morphology using the Xparticle software from Thermo Scientific. Powder morphology was assessed based on the aspect ratio, where an aspect ratio of 1 signifies ideal powder sphericity. The analysis of the composite structure of the powder involved determining the content of SiC particles in the powder particles. This was achieved by embedding the powder particles and grinding them using silicon carbide papers with grit sizes from 600 to 2500. Subsequently, they underwent oxide-polishing (0.05 µm silica solution, Struers OP-S Suspension) using a vibratory polishing machine. The prepared powder samples were imaged with a scanning electron microscope (SEM) equipped with a Back-Scattered Electron (BSE) detector. The content of SiC particles in the powder particles was manually determined using ATLAS Software, employing a method based on color contrast differences.

Processability of AMC powders.

The efficiency of the ultrasonic atomization process depended on the type of heat source used to melt the initial material (see Fig. 2a). Utilizing induction and plasma enabled the achievement of a relatively high process efficiency exceeding 40%. However, when using an arc as the heat source, the process efficiency was possible only at a level of 15%. In the case of plasma and arc heat sources, based on a similar procedure for melting the feed material, a decrease in process efficiency occurred at the same stage of the process. Instabilities appeared during the melting stage, leading to the detachment of irregular large fragments of material, as illustrated by the example of plasma melting (see Fig. 3). Consequently, this disruption led to interference in surface coverage with molten material on the sonotrode, ultimately resulting in the formation of scrap. Although the material exhibited similar behavior during melting with both heat sources, the efficiency of the process was notably lower when using the arc, at a level of 15%, compared to plasma, which achieved 41%.

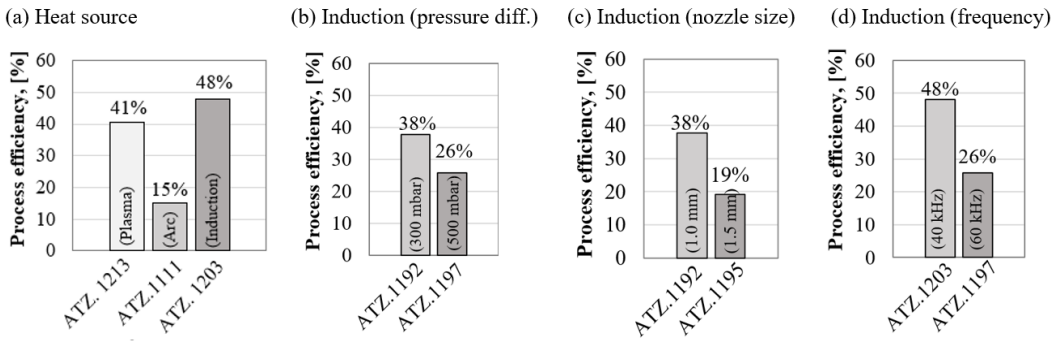

Fig. 2: A graphical representation of how the efficiency of particle production is affected by the process parameters. The efficiency of the ultrasonic atomization process is dependent on (a) the heat source, and when utilizing induction, in dependant on (b) pressure difference, (c) nozzle size, and (d) frequency.

These differences arise from fundamental variances in the melting processes of the material using arc and plasma. In arc melting, the flow of electrical current is destabilized by the introduction of the feedstock material from AMC containing poorly conductive SiC particles. The similar instabilities of the arc plasma were detailed described by the same type of ceramic powder [9]. Conversely, plasma melting of the feed material occurs without direct contact. As a result, the SiC particle content in the feed material is not directly linked to the plasma, making this process more stable compared to arc melting.

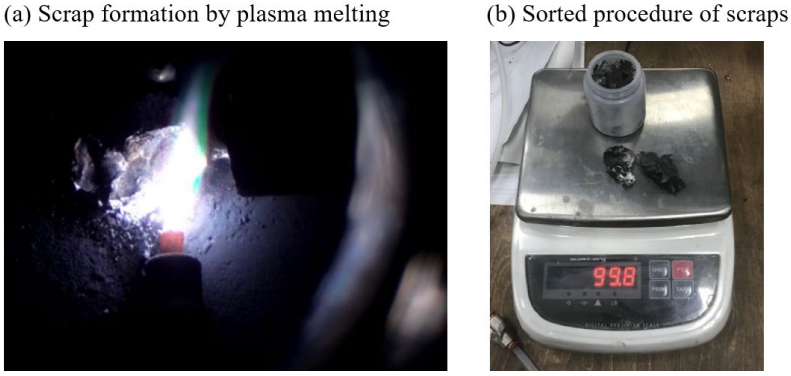

Fig. 3: (a) Scrap formation during the atomization process using plasma melting, and (b) the sorted procedure of scraps from the AMC powder.

The atomization process demonstrates its highest efficiency when employing induction, surpassing that of plasma and arc melting methods (see Fig. 2a). This method, employing a distinct procedural approach compared to other heat sources in this study, faces unique challenges in achieving a one-to-one ratio of AMC powder to feed material. Primarily, it was crucial to pour the material quickly to prevent alloy segregation and achieve a composite structure. Therefore, to influence the flow rate of AMC material, two parameters were varied: the pressure difference and the size. This assumption was based on the idea that an increase in material flow rate could be achieved by increasing either of these two parameters. However, the results show that utilizing a higher-pressure difference of 500 mbar compared to 300 mbar to a decrease in process efficiency from 38% to only 26% (see Fig. 2b). A similar effect was observed when increasing the nozzle size. The process efficiency dropped by half from 38% to 19% when the nozzle size was increased from 1.0 mm to 1.5 mm (see Fig. 2c).

Fig. 4: (a) High-volume material flow during atomization, (b) Unprocessed material in crucible after process, (c) Visible segregation of SiC from AlSiMg in the unprocessed material.

The decrease in efficiency in the case of pressure difference and nozzle size for induction melting was likely caused by two different effects. The first effect was the excessive volume of poured material for the ultrasonic system to handle. As a result, most of the molten AMC material fell from the ultrasonic system as large drops, failing to undergo atomization, as can be seen in Fig. 4a. The second effect was clogging or a reduction in flow rate from the spout to the drips. In Fig. 4b, an example of unprocessed material remaining in the crucible after the process is depicted, resulting from nozzle clogging. This procedural complication significantly extended the process time and caused further segregation of SiC from AlSiMg, as can be observed in the Fig. 4c depicting the solidified unprocessed material with visible SiC segregation from AlSiMg. The process observations indicate that, in the case of composites, the size of reinforcement is crucial for the size of the spout. However, it is advisable to use the smallest size of nozzle that allows for optimal pouring of the material. Furthermore, the results show that the efficiency of ultrasonic atomization process using induction melting is closely dependent on the frequency of the vibration plate (see Fig. 2d). Utilizing a 40 kHz transducer resulted in nearly double the efficiency compared to a 60 kHz transducer. The lower frequency facilitated the application of higher ultrasonic parameters, aiding in releasing droplets from the melt for subsequent solidification into powder particles.

Properties of AMC Powders.

The analysis of the produced AMC powders revealed specific correlations between powder properties and process conditions. Significant differences were noted in terms of morphology and particle size. Considering this, the morphology of AMC powders varied depending on the heat source used to melt the initial material (see Fig. 5a).

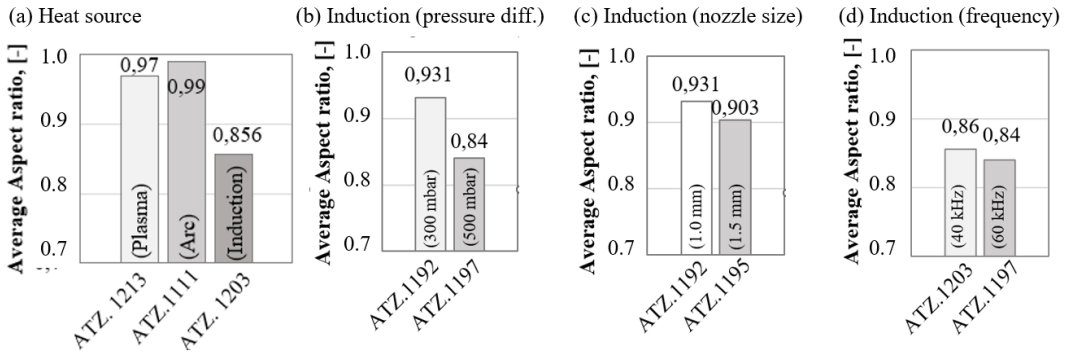

Fig. 5: A graphical representation of how the aspect ratio of particles is affected by the process parameters. The average aspect ratio of the AMC powder is dependent on (a) the heat source, and when utilizing induction, in dependant on (b) pressure difference, (c) nozzle size, and (d) frequency.

AMC powder produced by plasma and arc melting attained the highest aspect ratio of nearly 1.0, signifying nearly ideal sphericity. The aspect ratio of AMC powder produced by induction melting was significantly below 0.9, revealing a deviating powder sphericity. The cause of the specific aspect ratio can be understood by analyzing SEM images presenting AMC powder atomized using various heat sources. The AMC powder produced by arc melting exhibited an almost ideal spherical form (see Fig. 6b). In the case of AMC powders produced by plasma and induction melting (see Fig. 6a,c), some powder particles displayed an elongated shape, fractures, agglomeration, or satellites. However, the content of powder particles with morphological deviations was significantly higher in the case of AMC powder produced by induction compared to plasma melting.

When employing induction melting with various process parameters, a notable distinction in powder morphology was evident solely in relation to the pressure difference (see Fig. 5b-d). At a lower pressure difference of 300 mbar, the aspect ratio reached 0.93, whereas at a higher pressure difference of 500 mbar, it decreased to 0.84. The direct impact of frequency or nozzle size on powder size could not be precisely determined, as adjustments to these parameters resulted in minimal changes in aspect ratio. Both frequencies of 40 and 60 kHz yielded an aspect ratio of approximately 0.84. Similarly, for nozzle size, an aspect ratio of 0.91 was observed for both 1.0 mm and 1.5 mm sizes.

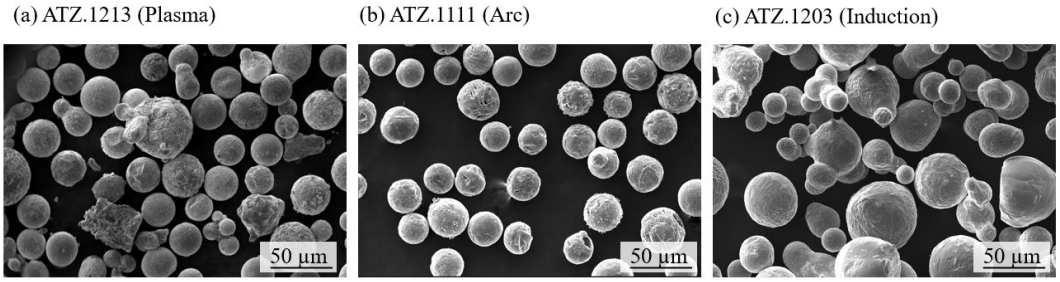

Fig. 6: SEM images of AMC powder atomized using (a) Plasma, (b) Arc and (c) Induction melting.

The powder size varied also depending on the heat source used to melt the initial material (see Fig. 7). AMC powder produced by induction melting achieved the highest average powder size of 170 µm. In contrast, the average size of AMC powder produced by arc and plasma melting was significantly smaller, reaching approximately 90 µm. In the case of various process parameters using induction melting, a significant difference in powder size was only observed for the frequency. At a low frequency of 40 kHz, the powder size reached a value of 170 µm. In comparison, the powder size at the high frequency of 60 kHz was only 120 µm. The direct influence of pressure difference or nozzle size on the powder size could not be precisely determined, as changing these parameters resulted in minimal alterations in powder size. For both pressure differences of 300 and 500 mbar, the powder size was approximately 110 µm. The same effect was observed for nozzle size, where the powder size of 100 µm was defined for both nozzle sizes of 1.0 and 1.5 mm.

The SiC particle content in the AMC powder was found to be very low after all atomization processes. In the case of arc and induction melting, the SiC content was only 3.5%, while with plasma, it was approximately 2% (see Fig. 8). Additionally, the variation of parameters for induction melting did not significantly ensure the desired content of SiC particles in the powder matrix (see Fig. 8b-c).

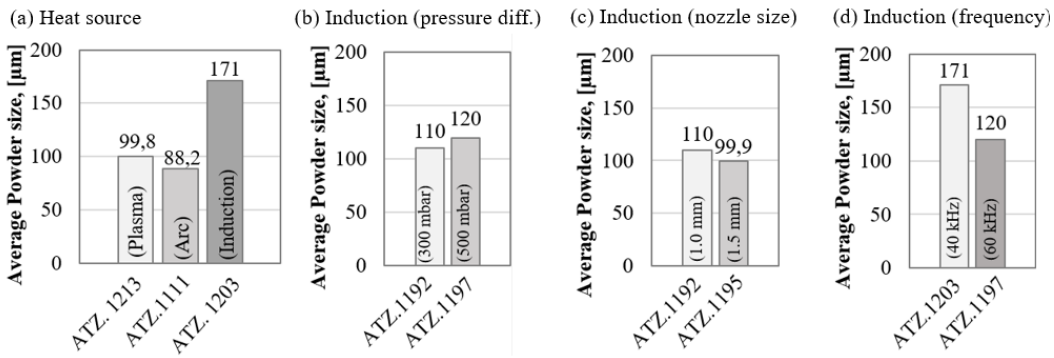

Fig. 7: A graphical representation of how the particle size is affected by the process parameters. The content of SiC particles in AMC powder is dependent on (a) the heat source, and when utilizing induction, is dependent on the (b) pressure difference, (c) nozzle size, and (d) frequency.

The main reason for the deviating composite structure achieved by arc and plasma melting is the dissolution of SiC particles due to the high temperature of both heat sources during the melting of the feed material [10]. In the case of induction melting, the low content of SiC particles in the AMC powder after the induction melting process may result from the melting temperature, as SiC can react with molten Al alloy at temperatures ranging from 667°C to 1347°C [10]. However, it is presumed that the more likely reason for the low SiC content in the AMC powder is process-related effects, such as (1) insufficient material flow leading to segregation or (2) excessively fast material flow resulting in unprocessed material due to nozzle clogging.

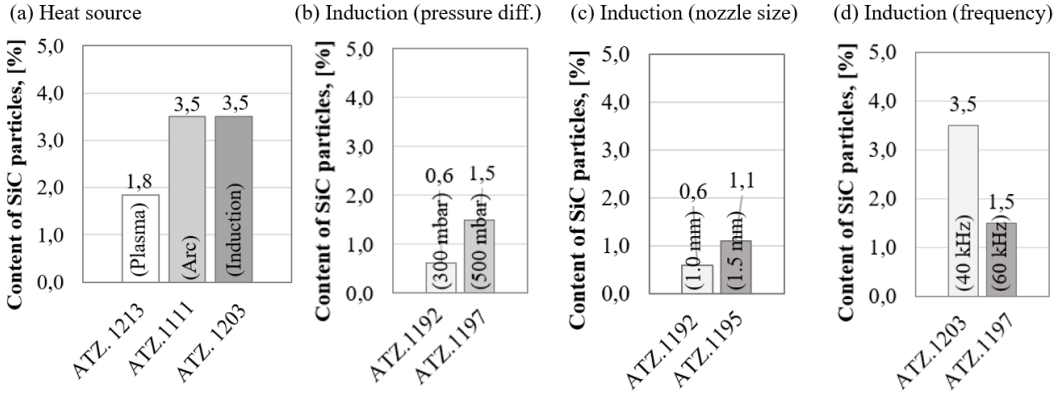

Fig. 8: A graphical representation of how the content of SiC in powder matrix is affected by the process parameters. The average size of the AMC powder is dependent on (a) the heat source, and when utilizing induction, is dependent on (b) pressure difference, (c) nozzle size, and (d) frequency.

Summary

In the present work, AMC powder, comprising AlSi9Mg reinforced with SiC particles, was produced employing ultrasonic atomization technology under varied process conditions. The following conclusions can be drawn:

- The efficiency of the ultrasonic process for producing AMC powder depended on the selected heat source. The highest process efficiency (almost 50%) was achieved with the induction system. Further improvement of the efficiency for this heat source required overcoming determined process challenges.
- The morphology of ultrasonically atomized powders was similar for all utilized heat sources, with an aspect ratio above 0.93, indicating high powder sphericity. In the case of induction melting, a correlation between pressure difference and aspect ratio was determined.

- The average size of AMC powder produced by all heat sources was comparable, ranging from 88.2 to 120 µm, while the high frequency in the case of induction resulted in an increased powder size of up to 170 µm.
- The content of SiC particles in the produced AMC powders was very low for all applied process conditions. In the case of arc and plasma melting, the likely reason for this effect is the dissolution of the SiC particles due to the high temperature of both heat sources. In contrast, the low SiC content in the AMC powders resulted from a process challenge, including the compensation of material flow to avoid segregations of SiC from the aluminum alloy and the lack of material processing due to nozzle clogging.

Ultrasonic atomization with induction melting has the greatest potential for processing AMC powder due to its low temperature, which prevents the dissolution of SiC particles. An increase in process efficiency is possible with more trials and process optimization. However, achieving a composite structure through induction requires further development of the current setup, for example, by introducing a stirring device that could help in mixing both components.

References

[1] P. Garg, A. Jamwal, D. Kumar, K. K.Sadasivuni, C. M. Hussain, P. Gupta, Advance research progresses in aluminium matrix composites: Manufacturing & applications. Journal of Materials Research and Technology, 2019, 8(5):4924–39. https://doi.org/10.1016/j.jmrt.2019.06.028

[2] C. Y. Liu, Q. Wang, Y. Z. Jia, B. Zhang, R. Jing, M. Z. Ma, Q. Jing, R. P. Liu, Effect of W particles on the properties of accumulatively roll-bonded Al/W composites, Mater. Sci. Eng. A 547, 2012, 120e124. https://doi.org/10.1016/j.msea.2012.03.095

[3] S. Kobayashi, N. Hosodaa, R. Takashimab, Tungsten alloys as radiation protection materials, Nucl. Instrum. Methods Phys. Res. 390, 1997, 426e430.

[4] V. V. Cherdyntsev, M. V. Gorshenkov, V. D. Danilov, S. D. Kaloshkin, V. N. Gul'bin, Metal-matrix radiation-protective composite materials based ON aluminum, Met. Sci. Heat Treat. 55 ,2013, 14e18. https://doi.org/10.1007/s11041-013-9571-2

[5] X. Xi, B. Chen, C. Tan, X. Song, J. Feng. Microstructure and mechanical properties of SiC reinforced AlSi10Mg composites fabricated by laser metal deposition. Journal of Manufacturing Processes, 2020, 58(17):763–74. https://doi.org/10.1016/j.jmapro.2020.08.073

[6] https://www.amazemet.com/repowder

[7] A. Jedynak. G. Gökhan, A. Neumann, P. Robert, S. Härtel. Semi-finished powder of aluminum matrix composite for a direct energy deposition additive manufacturing. Material Research Proceedings 28, 2023, 199-206

[8] M. Graf. New casting process for the production of AMCs with high volume content of einforced particle phase. Proceedings 5th IMTC 2021.

[9] J. Sun, H. Yu, D. Zeng, P. Shen. Wire–powder–arc additive manufacturing: A viable strategy to fabricate carbide ceramic/aluminum alloy multi-material structures, Additive Manufacturing, Volume 51, 2022, 102637, ISSN 2214-8604, https://doi.org/10.1016/j.addma.2022.102637

[10] J. Chen, R. Zhang, B.S. Amirkhiz, H. Gu, Synthesis of In Situ SiC/Graphite/Al Hybrid Composite Coating by Laser Direct Energy Deposition, Metall. Mater. Trans. A 53 (2022) 484–502. https://doi.org/10.1007/s11661-021-06508-x